

# THE AMERICAN MINERALOGIST

JOURNAL OF THE MINERALOGICAL SOCIETY OF AMERICA

Vol. 35

MAY-JUNE, 1950

Nos. 5 and 6

## Contributions to Canadian Mineralogy

Volume 5, Part 2

*Sponsored by The Walker Mineralogical Club*

*Edited by M. A. Peacock, Toronto*

### DESCRIPTION AND SYNTHESIS OF THE SELENIDE MINERALS\*

J. W. EARLEY

*Gulf Research & Development Company, Pittsburgh, Pennsylvania*

#### CONTENTS

Abstract . . . . .	338
Introduction . . . . .	338
Methods of Study . . . . .	338
Material and Acknowledgments . . . . .	340
Mineral Descriptions and Syntheses . . . . .	340
Naumannite . . . . .	340
Aguilarite . . . . .	343
Eucairite . . . . .	345
Crookesite . . . . .	347
Berzelianite . . . . .	351
Umangite . . . . .	354
Clausthalite . . . . .	356
Tiemannite . . . . .	358
Klockmannite . . . . .	360
Penroseite . . . . .	360
Other Selenides . . . . .	362
Guanajuatite . . . . .	362
Paraguanajuatite . . . . .	362
Classification . . . . .	362
References . . . . .	364

\* Contributions to Mineralogy from the Department of Geological Sciences, University of Toronto, 1950, no. 1.

Extracted from a thesis to be submitted for the degree of Ph.D., *University of Toronto* (Toronto, Canada). Published with the permission of the Research Council of Ontario and the Gulf Research & Development Company.

## ABSTRACT

A study of natural and artificial selenides, mainly by microscopic and *x*-ray methods, has led to revised descriptions of the selenide minerals. The mineral descriptions contain some new measurements of specific gravity, new unit cell dimensions (notably for eucairite, crookesite, and umangite), together with *x*-ray powder data for all the species and reproductions of the patterns. The classification of the selenides given in Dana (1944) is modified by the addition of a tetragonal group to the  $A_2X$  type, and the recognition of an  $A_{2-z}X$  type.

## INTRODUCTION

In 1818 Berzelius (Dana, 1944, p. 182) announced the discovery of the new element selenium simultaneously with the recognition of two selenide minerals now known as berzelianite and eucairite. Most of the additional selenide minerals known today were recognized and briefly described in the following three decades, and relatively little has been added to the knowledge of these minerals in the past century.

The telluride minerals, recently described by Thompson (1949), are rare and little known as compared to the sulphides, and the selenides bear a similar relation to the tellurides. As a group, the selenides are exceedingly uncommon in occurrence and they appear almost invariably in minute amounts, entirely lacking in crystal form, and intimately associated with various selenides and other ores. In consequence the crystallographic information is particularly incomplete on these minerals and their physical and chemical properties are not well known.

The known localities for the selenide minerals are primarily Skrikerum (Sweden), Harz Mountains (Germany), and Sierra de Umango (Argentina). Although the element selenium is recovered in notable quantities from the smelters at Sudbury and Noranda, the source of the selenium is not known. In 1949 Dr. E. W. Nuffield, University of Toronto, noted clausenthalite,  $PbSe$ , in a suite of ore specimens from Theano Point (Ontario), and Mr. S. Kaiman, Bureau of Mines, Ottawa, has identified selenide minerals in ore specimens from Lake Athabaska (Northwest Territories); but beyond these occurrences nothing is known of the distribution of selenide minerals in Canada.

## METHODS OF STUDY

The study of each mineral commenced with a macroscopic examination of hand specimens. This, coupled with a binocular-microscopic study, disclosed such physical properties as colour on fresh and tarnished surfaces, cleavage, fracture, hardness, and tenacity. Where possible, single crystal fragments were carefully chosen for specific gravity determinations using the Berman balance. A fragment or group of fragments weighing from 10–20 milligrams gave the most satisfactory results.

Since all selenide minerals are opaque, polished sections of each mineral were prepared for microscopic study in reflected light. This examination revealed such properties as colour, reflection pleochroism, polarization effects, and the Talmadge hardness estimated with a needle. In addition, the polished mineral surfaces were treated with standard etching reagents as used by Short (1940).

To obtain specific crystallographic information it was necessary, except with the cubic species, to use single crystal  $x$ -ray methods which yielded the symmetry and dimensions of the unit cell. With the selenides, which rarely show crystal form or display good cleavage, the search for a suitable single crystal is a long and tedious and sometimes fruitless procedure. Fragments showing only one or two poorly developed faces were oriented crystallographically as well as possible, firstly, using the optical goniometer and secondly by a series of rotation photographs coupled with minor adjustments of the  $x$ -ray goniometer head. The cell dimensions in kX units ( $\lambda\text{CuK}\alpha_1=1.5374$  kX) and the measured specific gravity of the mineral, with the mass factor 1.650, gave the molecular weight of the cell contents and in turn the calculated density. To complete the mineral description an  $x$ -ray powder pattern was taken as a "fingerprint" of the species. The tabulated powder data include the observed relative intensities and glancing angles for  $\text{CuK}\alpha_1$  radiation, together with the measured spacings, in kX, and when possible the indices of the powder lines and the calculated spacings, establishing a standard  $x$ -ray powder pattern with every line accounted for or proved to be extraneous. These standard patterns served to compare known and doubtful materials, and to identify unknown materials.

Since the selenides often occur in small amounts, closely associated with other selenides, sulphides, and their alteration products, it is often difficult to identify with certainty the rarer species using standard microscopic methods, and in such circumstances it is imperative to use the  $x$ -ray powder method. The procedure used to obtain  $x$ -ray powder photographs from small areas of a particular mineral in a polished section is essentially the same as that described by Thompson (1949, p. 344).

With a view to obtaining relatively abundant material of known composition on which to verify crystallographic, physical, and microscopical properties, an attempt was made to reproduce all the known selenide minerals and certain possible isostructural series by pyrosyntheses. For this purpose the pure powdered elements were weighed out in charges of 1–2 grams, intimately mixed, and introduced into silica glass tubes of about 2 cc. capacity, which had been closed at one end and drawn out to a narrow neck at the other. The tubes were evacuated, sealed off and heated with a Bunsen or hotter flame to produce fusion and combination

of the elements. After cooling, the tubes were broken and the practically homogeneous plugs were broken into two, one part being mounted for a polished section, the other retained for  $x$ -ray and other observations and for reference. By this simple method artificial compounds were obtained, identical or sometimes only similar to the corresponding minerals.

#### MATERIAL AND ACKNOWLEDGMENTS

For the many excellent selenide specimens which were made available, my thanks are due to Dr. V. B. Meen, the Royal Ontario Museum of Geology and Mineralogy, Toronto, Ontario; to Dr. C. Frondel, Harvard Mineralogical Museum, Cambridge, Mass.; to Dr. E. P. Henderson, United States National Museum, Washington, D. C., and to Dr. L. G. Berry, Queen's University Museum, Kingston, Ontario. The author wishes to thank Professor M. A. Peacock for the use of several fine selenide specimens kindly provided by Dr. Frans Wickman, Stockholm, Sweden, and Professor P. Ramdohr, Berlin, Germany.

Professor Peacock gave generously of his time supervising this study and assisting in the preparation of this report. The writer is also indebted to Dr. F. G. Smith, Dr. E. W. Nuffield, and Mr. A. R. Graham for constructive discussion of various problems.

The Research Council of Ontario awarded generous scholarships to the author, making it possible to carry out this study in the Mineralogical Laboratories of the Department of Geological Sciences, University of Toronto.

#### MINERAL DESCRIPTIONS AND SYNTHESSES

##### Naumannite— $Ag_2Se$

Naumannite with clausthalite and chalcopyrite in carbonate gangue, from Tilkerode, Harz, Germany; ore specimen and polished section provided by Professor P. Ramdohr (Berlin).

»»»→

FIG. 1. Naumannite (medium grey) and clausthalite (light grey) in a veinlet partly rimmed by chalcopyrite in carbonate gangue; Tilkerode, Harz mountains, Germany.

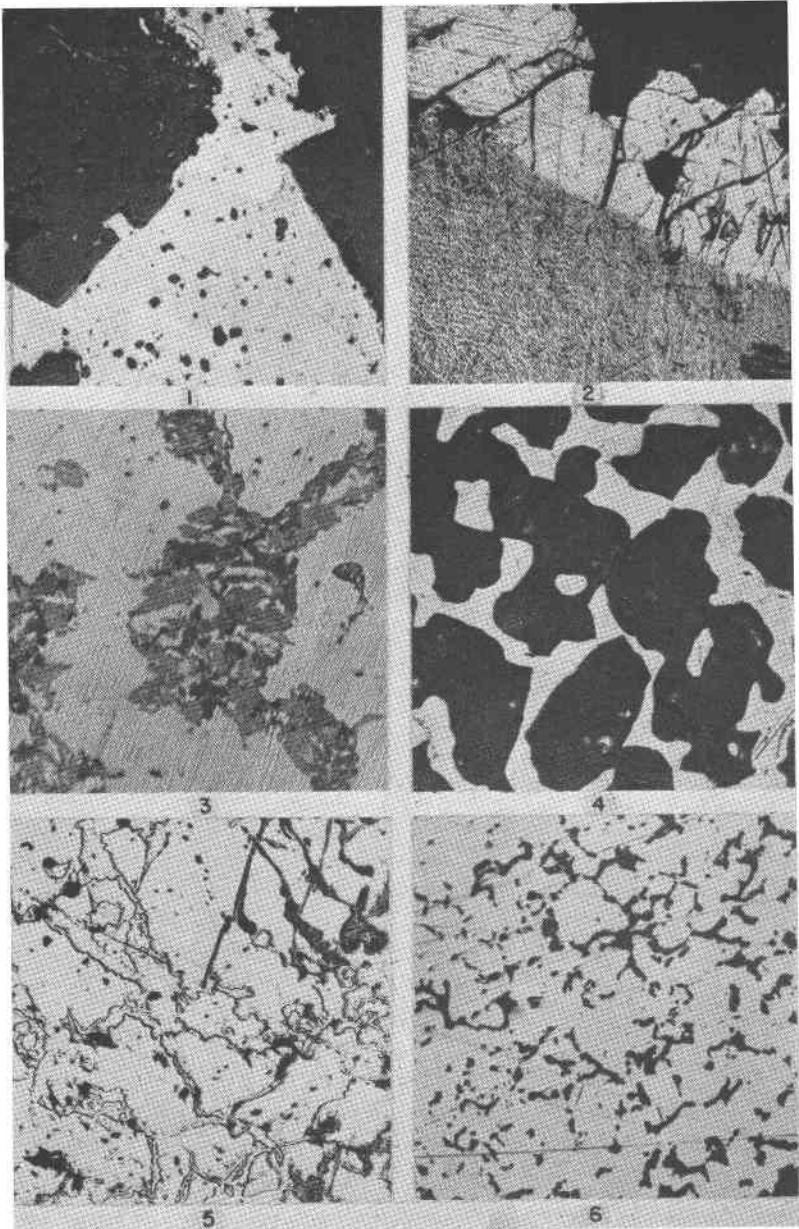
FIG. 2. Aguilarite (medium grey) and pearceite (light grey) in calcite gangue; Guanaajuato, Mexico.

FIG. 3. Umangite (dark grey) in groundmass of eucairite (medium grey); Sierra de Umango, Argentina.

FIG. 4. Eucairite (light grey) in carbonaceous and siliceous gangue, sieve-like texture; Skrikerum, Sweden.

FIG. 5. Penroseite (light grey) cut by veinlets of clausthalite (grey-white); Colquechaca, Bolivia.

FIG. 6. Eucairite (light grey) intimately intergrown with chalcomenite (dark grey); Sierra de Umango, Argentina.



FIGS. 1-6. Photomicrographs of some selenide minerals. 1 nicol;  $\times 70$ ; full size reproductions of contact prints.

The selenides appear intimately intergrown in minute veinlets in the gangue, naumannite being hardly distinguishable from clausthalite even under the binocular. Naumannite is slightly more lustrous than clausthalite and its colour is greyish iron-black tarnishing in time to brownish iridescent, in contrast with the lead-grey of clausthalite. Naumannite is somewhat sectile with a poor hackly fracture. No cleavage was observed, and clean fragments of sufficient size for a specific gravity measurement could not be obtained.

In the polished section (Fig. 1) naumannite is grey (between argentite and tetrahedrite in colour), and darker than clausthalite, with no evidence of cleavage or parting. Anisotropism is distinct but weak (light grey to dark grey) and indications of mimetic twinning (Schneiderhöhn & Ramdohr, 1931) were not observed. Satisfactory etch tests could not be made. The Talmadge hardness is B.

Naumannite gave a complex  $x$ -ray powder pattern (Fig. 9 and Table 1) which cannot be indexed on a cubic lattice. The pattern compares in complexity with that of acanthite, which is monoclinic (pseudo-orthorhombic) according to Ramsdell (1943, p. 401), but the material offered no chance of single-crystal photographs for a determination of the unit cell. The cubic mineral identified as naumannite associated with penroseite from Colquechaca, Bolivia (Bannister & Hey, 1937, p. 319) is probably clausthalite.

The compound  $\text{Ag}_2\text{Se}$  was prepared by fusing the powdered elements in the proper atomic proportions in an evacuated silica glass tube. The charge fused readily to a bright metallic globule and cooled to a compact steel-grey regulus. Three fragments gave  $G = 7.69-7.79$  which compares with 7.87 calculated for cubic  $\text{Ag}_2\text{Se}$ , 7.0-8.0 measured on naumannite (Dana, 1944, p. 179). In polished section the product is grey and homogeneous, with a few minute voids. It shows weak reflection pleochroism and moderate anisotropism (faint brown to pale blue) without indications of twinning or parting. Etch reactions:  $\text{HNO}_3$  (1:1) stains light brown in 2 minutes;  $\text{HCl}$  (1:1) negative;  $\text{KCN}$  stains faint brown after 2 minutes;  $\text{FeCl}_3$  instantly stains iridescent, bringing out texture;  $\text{KOH}$  negative,  $\text{HgCl}_2$  quickly stains iridescent, bringing out scratches. These reactions are almost the same as those given for naumannite by Short (1940, p. 135). The  $x$ -ray powder pattern (Fig. 10) is substantially the same as that of naumannite.

These observations show that naumannite is natural  $\beta$ - $\text{Ag}_2\text{Se}$ , the non-cubic phase which is stable below  $122^\circ-133^\circ$  C. (Rahlf's, 1936, p. 157). It seems certain that the early reported good cubic cleavage (Rose, 1828) was actually that of the abundant associated and intergrown clausthalite, and the later allusions to cleavage traces might be due to

parting associated with the  $\alpha$ - $\beta$  inversion. It remains to determine the unit cell of naumannite and eventually the structure.

TABLE 1. NAUMANNITE,  $\beta$ -Ag<sub>2</sub>Se: X-RAY POWDER PATTERN

<i>I</i>	$\theta$ (Cu)	<i>d</i> (meas.)	<i>I</i>	$\theta$ (Cu)	<i>d</i> (meas.)	<i>I</i>	$\theta$ (Cu)	<i>d</i> (meas.)
2	10.7°	4.14	$\frac{1}{2}$	29.6°	1.556	$\frac{1}{2}$	47.6°	1.041
$\frac{1}{2}$	11.8	3.76	1	30.8	1.501	$\frac{1}{2}$	49.6	1.009
1	13.5	3.29	$\frac{1}{2}$	31.5	1.471	$\frac{1}{2}$	50.3	0.999
1	15.5	2.88	2	32.35	1.437	$\frac{1}{2}$	52.05	0.975
1	16.5	2.71	$\frac{1}{2}$	33.6	1.389	$\frac{1}{2}$	53.85	0.952
10	16.8	2.66	1	34.95	1.342	$\frac{1}{2}$	55.2	0.936
10	17.45	2.56	1	35.6	1.321	$\frac{1}{2}$	55.75	0.930
2	18.55	2.42	$\frac{1}{2}$	36.2	1.302	$\frac{1}{2}$	57.35	0.913
6	20.15	2.23	$\frac{1}{2}$	37.45	1.264	$\frac{1}{2}$	57.85	0.908
2	21.4	2.11	2	38.3	1.240	$\frac{1}{2}$	59.05	0.896
2	21.75	2.07	$\frac{1}{2}$	39.4	1.211	$\frac{1}{2}$	59.9	0.889
4	22.6	2.00	$\frac{1}{2}$	40.2	1.191	$\frac{1}{2}$	61.0	0.879
$\frac{1}{2}$	23.4	1.936	$\frac{1}{2}$	41.05	1.171	$\frac{1}{2}$	63.1	0.862
2	24.3	1.868	$\frac{1}{2}$	42.35	1.141	$\frac{1}{2}$	69.15	0.823
1	25.05	1.816	$\frac{1}{2}$	43.25	1.122	$\frac{1}{2}$	71.05	0.813
1	26.65	1.714	$\frac{1}{2}$	44.55	1.096	$\frac{1}{2}$	71.85	0.809
1	27.5	1.665	$\frac{1}{2}$	45.85	1.071	$\frac{1}{2}$	75.15	0.795
2	28.6	1.606	$\frac{1}{2}$	46.65	1.057	$\frac{1}{2}$	77.75	0.787

#### Aguilarite—Ag<sub>4</sub>SeS

Aguilarite, Guanajuato, Mexico (Royal Ontario Museum of Geology and Mineralogy, M3832); skeleton dodecahedrons embedded in transparent calcite, partially coated with clayey material.

In daylight with a hand lens, aguilartite appears in clumps of intergrown rudely dodecahedral crystals with pitted surfaces and mostly rounded edges, filled with calcite and a brittle metallic mineral which gave the x-ray pattern of pearceite (Peacock & Berry, 1947, p. 12). The aguilartite is a bright lead-grey on a fresh surface while exposed surfaces are dull iron-grey to black; it is sectile and yields a hackly fracture with no evidence of cleavage. Specific gravity determinations on three individual crystal fragments range from 7.40 to 7.53 with the Berman balance. A second sponge-like specimen coated with siderite and labelled "aguilarite" from Guanajuato, Mexico, gave the x-ray powder pattern of acanthite, although the metallic constituent was physically similar to aguilartite but lacked the usual crystal form.

Aguilarite polishes somewhat unevenly, giving a micro-pitted surface with no evidence of cleavage or parting. The section (Fig. 2) is light grey with a very faint greenish tinge, slightly darker than argentite.

Anisotropism is distinct but very weak (shades of grey). The etch reactions are similar to those given by Short (1940, p. 128):  $\text{HNO}_3$  (1:1), light brown stain which is easily rubbed off, fumes tarnish a light brown;  $\text{HCl}$  (1:1), negative;  $\text{FeCl}_3$ , quickly stains iridescent;  $\text{HgCl}_2$ , quickly stains iridescent to black;  $\text{KCN}$ , leaves a light brown stain, easily rubbed off;  $\text{KOH}$ , negative. The Talmadge hardness is A.

Aguilarite gave a complex  $x$ -ray powder pattern (Fig. 7 & Table 2), distinctly different from those of naumannite and acanthite. The intensities and spacings agree substantially with those of Harcourt (1942, p. 69) and an attempt to index the pattern on a cubic lattice showed, as noted by Berman (Dana, 1944, p. 179), that this cannot be done. Since a single crystal fragment presumably represents the inversion product of a

TABLE 2. AGUILARITE,  $\beta$ - $\text{Ag}_4\text{SeS}$ : X-RAY POWDER PATTERN

<i>I</i>	$\theta(\text{Cu})$	<i>d</i> (meas.)	<i>I</i>	$\theta(\text{Cu})$	<i>d</i> (meas.)	<i>I</i>	$\theta(\text{Cu})$	<i>d</i> (meas.)
5	10.85°	4.09	1	24.1°	1.883	1	38.25°	1.242
1	12.0	3.70	1	26.55	1.720	1	39.05	1.220
2	15.8	2.83	1	29.15	1.578	$\frac{1}{2}$	44.85	1.090
2	17.05	2.62	1	29.85	1.545	$\frac{1}{2}$	47.75	1.038
2	17.3	2.58	1	31.55	1.470	$\frac{1}{2}$	48.25	1.030
10	18.5	2.42	1	32.65	1.425	$\frac{1}{2}$	53.25	0.959
6	20.5	2.19	1	34.65	1.353	$\frac{1}{2}$	54.05	0.950
2	21.8	2.07	1	36.1	1.305	$\frac{1}{2}$	60.35	0.855
2	22.95	1.971	1	36.7	1.286			

higher temperature cubic form, composed of individuals in random orientation, single crystal photographs for a unit cell determination seemed hopeless.

The compound  $\text{Ag}_4\text{SeS}$  was prepared by fusing the powdered elements in the proper proportions in an evacuated silica glass tube. The components fused readily to a bright metallic globule and cooled to a lead-gray regulus which had a very small amount of metallic silver in shiny particles adhering to the outer surface. A polished section of the product is homogeneous, grey, slightly porous and weakly anisotropic similar to aguilarite. The  $x$ -ray powder pattern of this compound (Fig. 8) is very similar to that of aguilarite.

These observations indicate that aguilarite corresponds to noncubic  $\beta$ - $\text{Ag}_4\text{SeS}$  which is stable at room temperature. The dodecahedral crystal form suggests inversion from cubic high temperature  $\alpha$ - $\text{Ag}_4\text{SeS}$ . Since the  $x$ -ray powder patterns of aguilarite and  $\text{Ag}_4\text{SeS}$  show only faint resemblances to those of naumannite,  $\text{Ag}_2\text{Se}$ , and argentite,  $\text{Ag}_2\text{S}$ ,



aguilarite is a distinct species and not merely a member of a naumannite-acanthite series, as suggested in Schneiderhöhn & Ramdohr (1931, p. 222).

**Eucairite—AgCuSe**

Eucairite, Skrikerum, Sweden (Natural History Museum, Stockholm, yellow 2345); disseminated blebs with severely tarnished surfaces in a serpentinized gangue of quartz and calcite.

Eucairite, Sierra de Umango, Argentina (United States National Museum, 84457); associated with umangite, chalcomenite, and malachite in a highly altered copper ore specimen.

Viewed with a hand lens, eucairite is a brilliant creamy white on a fresh surface, whereas exposed surfaces are bright bronze due to a tarnish that develops quickly. The mineral is brittle and fractures unevenly to subconchoidally with no evidence of cleavage. None of the material was satisfactory for specific gravity measurements.

Eucairite polishes to a smooth surface with no evidence of cleavage or parting (Figs. 4, 6). The polished surface appears tin-white with a faint creamy tinge. Reflection pleochroism is very weak with no obvious colour change, but with variable relief along grain boundaries. Anisotropism is strong with polarization colours olive-brown to steel-blue with a purplish tinge, somewhat less vivid than those given by Schneiderhöhn & Ramdohr (1931, p. 306). The etch reactions are essentially the same as those of Short (1940, p. 135):  $\text{HNO}_3$  (1:1), surface slowly stains greyish brown, fumes tarnish strongly brown to iridescent but rubs off;  $\text{HCl}$  (1:1), negative;  $\text{FeCl}_3$ , tarnishes iridescent to greyish blue;  $\text{KCN}$ , instantly stains brownish to black;  $\text{HgCl}_2$ , slowly yields a faint pinkish brown stain;  $\text{KOH}$ , negative. The Talmadge hardness is B.

A roughly equant fragment of eucairite was chosen from the Skrikerum specimen for single crystal measurements. The fragment was successfully oriented on the  $x$ -ray goniometer by a succession of rotation photographs and minor adjustments. Fairly good rotation and Weissenberg photographs gave the tetragonal cell dimensions:

$$a=4.075, c=6.29 \text{ kX}$$

Five very weak lines in the powder pattern (Table 3) can be explained by a triple  $c$ ; but since there is no evidence for this on the rotation photograph, these weak lines are evidently extraneous.

The Laue symmetry is  $4/mmm$  and the systematically missing spectra conform to the single condition:  $(hk0)$  present only with  $h+k=2n$ . This condition is compatible with the space group  $P4/nmm$ . With the cell contents  $2[\text{AgCuSe}]$  the calculated specific gravity is 7.91, as compared with the measured values 7.6–7.8 (Dana, 1944, p. 183).

Table 3 is based on the  $x$ -ray powder pattern (Fig. 11) of eucairite from Skrikerum, Sweden (NHM, Stockholm, yellow 2345). The measured spacings given by the ASTM (1945) cards do not agree well with those of our pattern.

A compound near  $\text{AgCuSe}$  in composition was prepared by fusing the elements in equal atomic proportions in a vacuum. The charge fused

TABLE 3. EUCAIRITE— $\text{AgCuSe}$ : X-RAY POWDER PATTERNTetragonal,  $P4/nmm$ ;  $a=4.075$ ,  $c=6.29$  kX;  $Z=2$ 

$I$	$\theta(\text{Cu})$	$d(\text{meas.})$	$(hkl)$	$d(\text{calc.})$	$I$	$\theta(\text{Cu})$	$d(\text{meas.})$	$(hkl)$	$d(\text{calc.})$
$\frac{1}{2}$	11.8°	3.76	—	—	1	39.75°	1.202	(015)	1.202
$\frac{1}{2}$	12.9	3.44	(011)	3.420				{(132)	1.192
1	14.15	3.14	(002)	3.145	1	40.15	1.192	{(124)	1.191
5	15.5	2.88	(110)	2.881				{(223)	1.187
7	17.1	2.61	(111)	2.620	$\frac{1}{2}$	42.65	1.135	(033)	1.140
4	18.05	2.48	(012)	2.490				{(125)	1.035
$\frac{1}{2}$	19.15	2.34	—	—	1	48.0	1.034	(034)	1.028
$\frac{1}{2}$	20.25	2.22	—	—				{(040)	1.019
10	21.25	2.12	(112)	2.125	$\frac{1}{2}$	49.0	1.019	(016)	1.015
2	22.35	2.02	(020)	2.038				{(035)	0.923
1	24.4	1.861	(013)	1.864	$\frac{1}{2}$	56.6	0.921	{(332)	0.919
$\frac{1}{2}$	26.8	1.705	{(022)	1.710				{(234)	0.918
			{(113)	1.695	$\frac{1}{2}$	57.55	0.911	(240)	0.911
$\frac{1}{4}$	28.25	1.624	—	—				{(126)	0.909
1	29.2	1.576	{(122)	1.577				{(135)	0.900
			{(004)	1.572	$\frac{1}{2}$	58.9	0.898	{(007)	0.899
$\frac{1}{2}$	29.95	1.540	—	—				{(143)	0.894
1	31.9	1.456	(023)	1.461				{(017)	0.877
$\frac{1}{2}$	33.95	1.376	{(114)	1.380	$\frac{1}{2}$	61.3	0.876	{(242)	0.875
			{(123)	1.375				{(333)	0.873
$\frac{1}{2}$	35.0	1.340	(031)	1.328	$\frac{1}{2}$	63.55	0.859	{(117)	0.858
$\frac{1}{2}$	35.75	1.316	(222)	1.310				{(044)	0.855
$\frac{1}{2}$	36.6	1.289	(130)	1.289				{(341)	0.808
$\frac{1}{2}$	37.35	1.267	(131)	1.262	$\frac{1}{2}$	72.55	0.806	{(051)	0.808
$\frac{1}{2}$	38.25	1.242	{(032)	1.247				{(127)	0.806
			{(024)	1.245					

readily to a shiny somewhat porous regulus. A freshly broken surface revealed a bright metallic product which is white with a distinct reddish buff tinge. After a week an exposed surface acquired a distinctly bronzy tarnish, eventually turning iridescent. A polished section of the regulus shows two constituents, one similar to eucairite making up about 95 per cent of the section, the other an intensely anisotropic product,  $\text{Cu}_3\text{Se}_2$  (umangite). An  $x$ -ray powder pattern of the dominant compound (Fig. 12) is similar to that of eucairite (Fig. 11).

These observations show that eucairite is tetragonal, in keeping with the strong anisotropism, and not isometric as suggested by Berzelius in 1818. The synthesis tends to confirm the accepted composition  $\text{AgCuSe}$  established from the analyses given in Hintze (1904).

**Crookesite**— $(\text{Cu,Tl,Ag})_2\text{Se}$

Crookesite, Skrikerum, Sweden; finely disseminated specks and small veinlets in translucent calcite with minor quartz.

Finely disseminated crookesite is localized in small areas giving the specimen a slaty, bluish black, mottled appearance. Individual particles of the mineral are not visible to the naked eye but can be seen with a binocular microscope. Crookesite is lead-grey on a fresh surface, brittle when crushed with a needle and shows two fairly well developed cleavages at right angles. A sufficiently large, pure sample could not be obtained for specific gravity measurements.

Crookesite polishes to a smooth surface and is distinctly grey, somewhat darker than argentite but lighter than tetrahedrite. Reflection pleochroism is imperceptible and the anisotropism is weak but clearly discernible (shades of grey). Due to the reactive nature of the carbonate gangue the etch reactions for  $\text{HNO}_3$ ,  $\text{HCl}$ , and  $\text{FeCl}_3$  are unreliable. The observed etch reactions are in fair agreement with those of Murdoch (Schneiderhöhn & Ramdohr, 1931, p. 302):  $\text{HNO}_3$  (1:1) fumes tarnish brown, rubs off;  $\text{HCl}$  (1:1) negative;  $\text{FeCl}_3$  negative;  $\text{KCN}$  negative;  $\text{HgCl}_2$  negative;  $\text{KOH}$  negative. The Talmadge hardness is C.

A fragment of crookesite ( $0.5 \times 0.3$  mm) showing two imperfect, mutually perpendicular cleavages was mounted for single crystal measurements. Good rotation and Weissenberg photographs gave tetragonal or pseudo-tetragonal unit cell dimensions:

$$a = 10.38, c = 3.92 \text{ kX}$$

Although the Weissenberg films show only monoclinic symmetry and the  $F$ -lattice type, with  $a = b = 10.38\sqrt{2} = 14.68 \text{ kX}$ ,  $\beta = 90^\circ$ , crookesite may be provisionally interpreted as pseudo-tetragonal with  $hkl$  present only with  $h+k+l=2n$ , leading to the possible space group  $I4/mmm$ . With reference to the pseudo-tetragonal unit cell the poorly developed cleavage is prismatic (020). The powder pattern of crookesite from Skrikerum (Sweden) (Fig. 13) has been indexed in this simpler manner (Table 4).

The composition of crookesite, known only through three early analyses by Nordenskiöld (1866, p. 366), is given as  $(\text{Cu, Tl, Ag})_2\text{Se}$ . Microchemical tests confirmed the presence of Cu, Ag, Se. In addition a small amount of crookesite dissolved in  $\text{HNO}_3$  yielded a character-

TABLE 4. CROOKESITE—(Cu,Tl,Ag)<sub>2</sub>Se: X-RAY POWDER PATTERN  
Pseudo-tetragonal, *I4/mmm*; *a* = 10.38, *c* = 3.92 kX; *Z* = 2

<i>I</i>	$\theta$ (Cu)	<i>d</i> (meas.)	( <i>hkl</i> )	<i>d</i> (calc.)	<i>I</i>	$\theta$ (Cu)	<i>d</i> (meas.)	( <i>hkl</i> )	<i>d</i> (calc.)
1	8.5°	5.20	(020)	5.190	$\frac{1}{2}$	30.15°	1.530	(332)	1.530
$\frac{1}{2}$	11.95	3.71	(220)	3.668	$\frac{1}{3}$	30.95	1.495	(451)	1.498
10	13.5	3.29	(130)	3.282	$\frac{1}{2}$	32.3	1.439	(361)	1.439
8	14.85	3.00	(121)	2.995				(460)	1.439
10	17.25	2.59	{(040)	2.595	1	35.65	1.319	(352)	1.318
			{(031)	2.594				(080)	1.322
1	18.4	2.44	(330)	2.447	1	37.75	1.256	(561)	1.252
			{(240)	2.321				(660)	1.223
3	19.35	2.32	{(231)	2.320	$\frac{1}{2}$	38.95	1.223	(181)	1.223
			{(141)	2.118				(471)	1.223
5	21.35	2.11	(002)	1.960	$\frac{1}{2}$	41.6	1.158	(480)	1.160
$\frac{1}{2}$	23.0	1.967	(440)	1.835				(462)	1.160
4	24.8	1.833	(350)	1.780	1	44.05	1.106	(091)	1.106
4	25.6	1.779	{(222)	1.729				(082)	1.082
$\frac{1}{2}$	26.45	1.726	{(060)	1.730	$\frac{1}{2}$	45.3	1.081	(671)	1.082
			{(251)	1.730				(282)	1.059
$\frac{1}{2}$	27.2	1.682	(132)	1.683	1	46.55	1.059	(581)	1.059
$\frac{1}{2}$	28.0	1.637	(260)	1.641					
1	29.45	1.563	{(161)	1.565					
			{(042)	1.564					

istic thallium-green flame. With a unit cell containing 24 atoms in the proportions of the analyses, Cu:Tl:Ag = 0.4569:0.1669:0.0510, or 8[Cu,Tl,Ag)<sub>2</sub>Se], the calculated specific gravity is 7.71, somewhat greater than the value given by Nordenskiöld (1866).

An attempt was made to prepare an artificial compound similar to crookesite by fusing appropriate proportions of Cu, Tl, Ag and Se in a

→→→→→

FIGS. 7-26. X-ray powder photographs with Cu/Ni radiation; Camera radius 90/π mm. (1°θ = 1 mm. on film); full size reproductions of contact prints.

FIG. 7. Aguilarite, Guanajuato, Mexico.

FIG. 8. Compound Ag<sub>4</sub>SeS formed by pyrosynthesis.

FIG. 9. Naumannite, Tilkerode, Harz Mountains, Germany.

FIG. 10. Compound Ag<sub>2</sub>Se formed by pyrosynthesis.

FIG. 11. Eucairite, Skrikerum, Sweden.

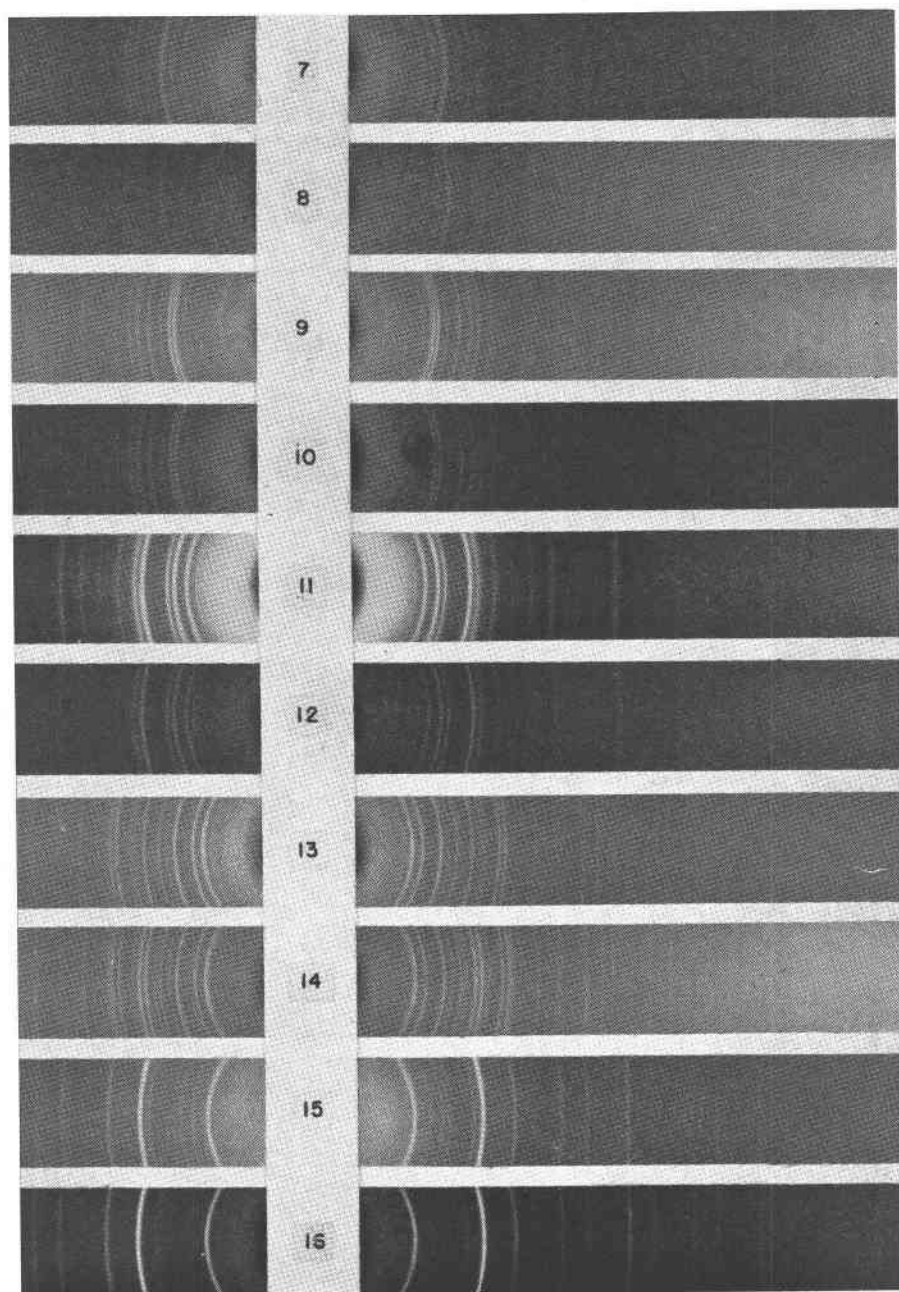
FIG. 12. Compound AgCuSe formed by pyrosynthesis.

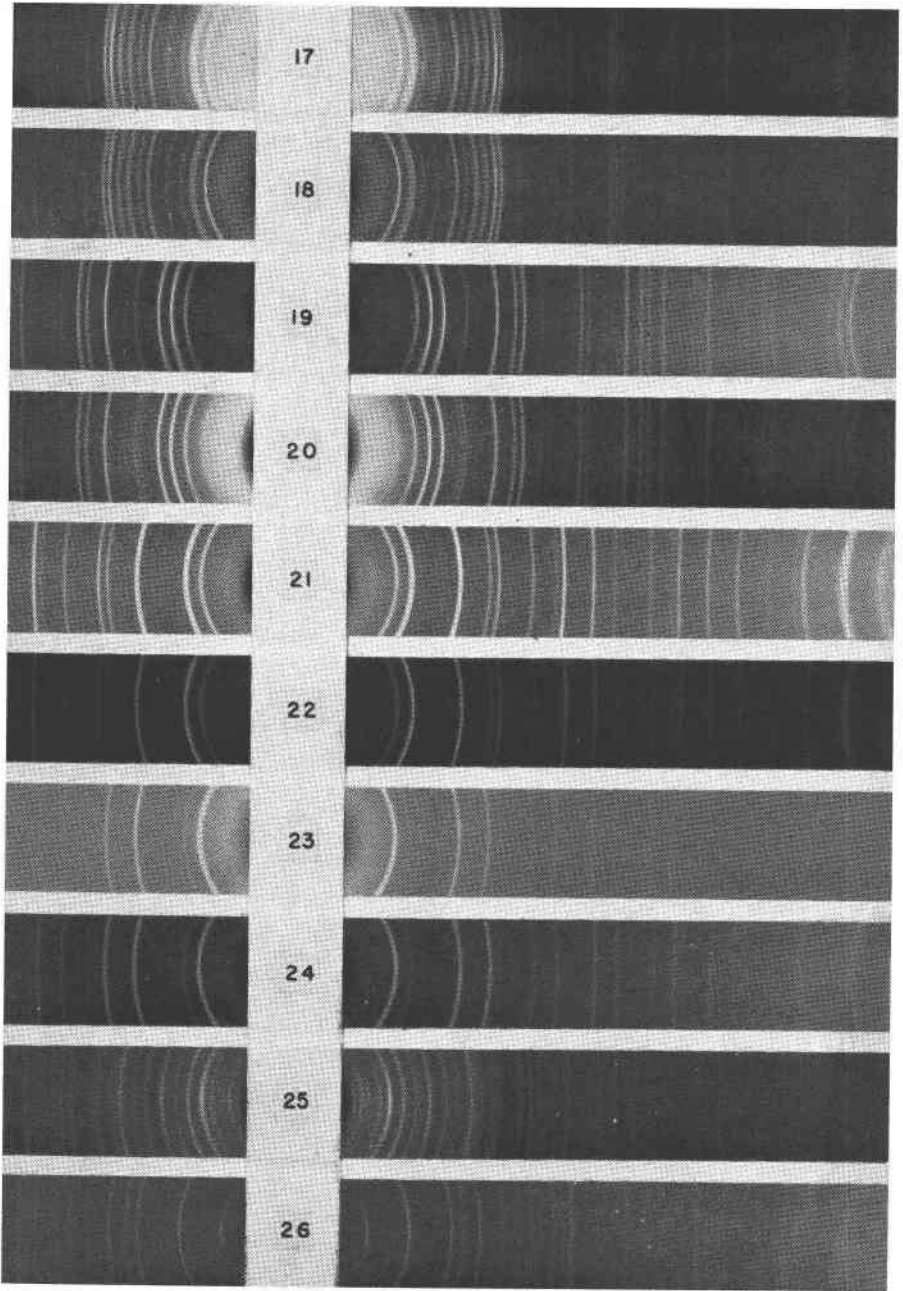
FIG. 13. Crookesite, Skrikerum, Sweden.

FIG. 14. Compound (Cu,Tl,Ag)<sub>2</sub>Se formed by pyrosynthesis.

FIG. 15. Berzelianite, Skrikerum, Sweden.

FIG. 16. Compound Cu<sub>2-x</sub> formed by pyrosynthesis.





vacuum. The elements fused with difficulty and ebullition of gas to a porous inhomogeneous mass. A polished section shows two products, the one resembling crookesite and the other, berzelianite. An  $x$ -ray powder pattern of the aggregate (Fig. 14) is similar to crookesite except for two diffraction lines which correspond to the two strongest lines of berzelianite.

These results show that crookesite is not cubic as suggested by Hiller (1940, p. 138); but it is interesting to note that the true monoclinic  $a = 14.68$  kX is almost identical with Hiller's cube edge 14.69 kX. The anisotropism and definite cleavage according to Ramdohr (in Hiller, 1940) are in good agreement with our observations.

#### Berzelianite— $\text{Cu}_{2-3}\text{Se}$

Berzelianite, Skrikerum, Sweden (Harvard Mineralogical Museum, 81739); finely disseminated in calcite gangue.

Berzelianite, Skrikerum, Sweden (ROM, M12324); finely disseminated in calcite gangue.

Berzelianite, locality unknown (Dept. of Geol., Univ. of Western Ontario); finely disseminated in calcite gangue.

Berzelianite, Aurora, Nevada, U.S.A.; disseminated in a highly weathered siliceous gangue associated with native gold and lead.

Berzelianite, Lake Athabaska, N.W.T., Canada (Bureau of Mines, Ottawa); blebs and veinlets in greyish pink calcite gangue associated with umangite and chalcocite.

Berzelianite appears as dusty black patches in otherwise translucent calcite associated with umangite, eucairite, and other selenides. With a binocular microscope, freshly fractured surfaces are shiny lead-grey with a faint bluish cast, somewhat less lustrous than clauthalite, while old surfaces are dusty metallic black. Berzelianite is brittle and fractures unevenly with no evidence of cleavage. Pure material could not be obtained in sufficient quantity for specific gravity measurements. However, specific gravity measurements of three independent fragments of pyrosynthetic material of composition  $\text{Cu}_{1.85}\text{Se}$  yielded an average value 6.65.



FIG. 17. Umangite, Sierra de Umango, Argentina.

FIG. 18. Compound  $\text{Cu}_3\text{Se}_2$  formed by pyrosynthesis.

FIG. 19. Penroseite, Colquechaca, Bolivia.

FIG. 20. Compound  $(\text{Ni,Cu})\text{Se}_2$  formed by pyrosynthesis.

FIG. 21. Clausthalite, Clausthal, Harz Mountains, Germany.

FIG. 22. Compound  $\text{PbSe}$  formed by pyrosynthesis.

FIG. 23. Tiemannite, Clausthal, Harz Mountains, Germany.

FIG. 24. Compound  $\text{HgSe}$  formed by pyrosynthesis.

FIG. 25. Guanajuatite, Guanajuato, Mexico.

FIG. 26. Compound  $\text{Bi}_2\text{Se}_3$  formed by pyrosynthesis.

In polished section berzelianite is steel-greyish white, isotropic, and without obvious cleavage traces. A smooth polished surface, in time, tarnishes bronzy iridescent. The etch reactions are similar to those given by Schneiderhöhn & Ramdohr (1931, p. 301):  $\text{HNO}_3$  (1:1), slowly stains iridescent with a reddish tinge;  $\text{HCl}$  (1:1), negative;  $\text{FeCl}_3$ , stains quickly light brown, rubs off;  $\text{KCN}$ , stains iridescent and finally black;  $\text{HgCl}_2$  stains slowly greyish black;  $\text{KOH}$ , negative. The Talmadge hardness is B.

An  $x$ -ray powder pattern of berzelianite (Fig. 15 & Table 6) from Skrikerum, Sweden (HMM, 81739) has been indexed on a cubic lattice:

$$a = 5.728 \text{ kX}$$

The spacings and intensities are in good agreement with those of Harcourt (1942, p. 72), and the cell edge agrees closely with previous measurements on berzelianite and artificial  $\text{Cu}_{2-x}\text{Se}$  (with  $x=0.2$ ); the cube-edge of  $\text{Cu}_2\text{Se}$  is slightly higher at room temperature and distinctly higher at about  $180^\circ \text{C}$ . (Table 5).

TABLE 5. BERZELIANITE,  $\text{Cu}_{2-x}\text{Se}$ , AND  $\text{Cu}_2\text{Se}$ : CUBE-EDGES

Berzelianite	$\text{Cu}_{2-x}\text{Se}$	$\text{Cu}_2\text{Se}$
—	—	5.751 Å (Davey, 1923)
5.731 Å	—	5.748 Å (Hartwig, 1926)
—	—	5.84 Å at $180^\circ \text{C}$ . (Rahlf's, 1936)
—	5.729 Å ( $x=0.2$ )	— (Borchert, 1945)
5.728 kX	5.74 kX ( $x=0.15$ )	5.81 kX at about $55^\circ \text{C}$ . (J.W.E.)

The systematically missing spectra are given by the conditions:  $hkl$  present only with  $h, k, l$ , all odd or all even,  $0kl$  present only with  $h+l=4n$ , leading to the space group  $Fd\bar{3}m$ . The calculated specific gravity with  $4[\text{Cu}_{2-x}\text{Se}]$  ( $x=0.15$ ) in the unit cell is 6.96, rather higher than the measured values,  $G=6.7$ , given by Berzelius (in Dana, 1892), and 6.65 on artificial material.

The following copper-selenium compounds were prepared by fusing known proportions of the elements in a vacuum:

$\text{Cu}:\text{Se}=32:16$ . The elements fuse with difficulty to a porous, steel-grey regulus which on breaking shows imperfect cubic cleavage. A section of the product is greyish white, homogeneous and isotropic. In a few weeks a polished surface develops a bronzy tarnish. An  $x$ -ray powder photograph of a random fragment yields a pattern similar to berzelianite but with each of the diffraction lines represented as doublets indicating a non-cubic lattice. However, an  $x$ -ray powder photograph taken at about  $55^\circ \text{C}$ . can be indexed as cubic with  $a = 5.81 \text{ kX}$ .



Cu:Se=30:16. The product appears macroscopically and microscopically similar to Cu:Se=32:16. The *x*-ray powder pattern of this material (Fig. 16) yields the berzelianite pattern with the exception of one very weak line which compares to one of the lines in the pattern of the former charge. The cube-edge is  $a=5.74$  kX.

Cu:Se=28:16. The elements fuse with less difficulty to a purplish black slightly porous regulus. A polished section of this compound appears homogeneous, faintly purplish grey and is isotropic. An *x*-ray

TABLE 6. BERZELIANITE— $\text{Cu}_{2-x}\text{Se}$ : X-RAY POWDER PATTERNCubic,  $Fd\bar{3}m$ ;  $a=5.728$  kX;  $Z=4$ 

<i>I</i>	$\theta(\text{Cu})$	<i>d</i> (meas.)	( <i>hkl</i> )	<i>d</i> (calc.)	<i>I</i>	$\theta(\text{Cu})$	<i>d</i> (meas.)	( <i>hkl</i> )	<i>d</i> (calc.)
$\frac{1}{2}$	12.65°	3.51	—	—	3	32.5°	1.431	(004)	1.432
9	13.4	3.32	(111)	3.308	2	35.8	1.314	(133)	1.315
1	15.55	2.87	(002)	2.864	4	41.1	1.169	(224)	1.170
*1	17.05	2.62	—	—	2	44.2	1.103	{(115)} {(333)}	1.103
* $\frac{1}{2}$	18.05	2.48	—	—	1	49.4	1.012	(044)	1.013
* $\frac{1}{2}$	19.95	2.25	—	—	1	52.65	0.967	(135)	0.968
*1	21.15	2.13	—	—	2	58.05	0.906	(026)	0.906
10	22.35	2.02	(022)	2.026	1	61.6	0.874	(335)	0.874
* $\frac{1}{2}$	23.8	1.905	—	—	$\frac{1}{2}$	68.5	0.826	(444)	0.827
* $\frac{1}{2}$	24.95	1.822	—	—	1	73.4	0.802	{(117)} {(155)}	0.802
* $\frac{1}{2}$	25.65	1.776	—	—					
8	26.45	1.726	(113)	1.728					

\* Extra lines due mainly to umangite.

powder photograph of a random fragment shows the berzelianite pattern with six extra lines characteristic of the umangite pattern. This component, which is normally intensely anisotropic, must be distributed in extremely minute areas in the polished section, producing no distinct anisotropism.

Cu:Se=27:16. The elements fused similarly to the charge. Cu:Se=28:16, producing a slightly porous, purplish regulus. A polished section of this material shows two phases, the one identical with Cu:Se=28:16, the other with Cu:Se=3:2 (umangite). The latter constituent occurs as elliptical inclusions in the groundmass. The *x*-ray powder pattern of a random fragment shows both umangite and berzelianite diffraction lines.

These observations show that berzelianite is cubic at ordinary temperatures and has a composition,  $\text{Cu}_{2-x}\text{Se}$ , representing a structure which is deficient in copper atoms as proposed by Borchert (1945). The homogeneous berzelianite phase appears to be slightly poorer in Cu than

Cu:Se=30:16, indicating the composition with  $x=0.15$  (Cu:Se=29.6:16), rather than  $x=0.2$  (Cu:Se=28.8:16) given by Borchert. The compound  $\text{Cu}_2\text{Se}$  has a non-cubic low temperature phase,  $\beta\text{-Cu}_2\text{Se}$ , which inverts at elevated temperatures to  $\alpha\text{-Cu}_2\text{Se}$  which is cubic, confirming the results of Rahlfs (1936).

#### Umangite— $\text{Cu}_3\text{Se}_2$

Umangite, Sierra de Umango, Argentina (ROM, E3249); massive ore specimen cut by veinlets of chalcomenite, malachite and calcite.

Umangite, Sierra de Umango, Argentina (Queen's University Museum of Geology and Mineralogy, A51a—1); massive ore specimen cut by veinlets of chalcomenite and malachite and having small inclusions of clausthalite.

"Berzelianite," Sierra de Cacheuta, Argentina (ROM, M12864); massive ore specimen cut by veinlets of chalcomenite and malachite.

"Berzelianite," Skrikerum, Sweden (QM, 491); finely disseminated specks in calcite, localized, giving a patchy appearance to the specimen, with minor chalcomenite and malachite.

"Klockmannite," Sierra de Umango, Argentina (USNM, R519); massive ore specimen cut by veinlets of clausthalite and chalcomenite.

"Berzelianite," Tilkerode, Germany (HMM, 81763); finely disseminated specks in a vein of calcite filling a fracture in dark siliceous rock.

On fresh surfaces umangite unlike any of the other selenides appears lustrous bluish black with a distinct reddish cast while weathered surfaces are a dull iridescent purplish colour. It is brittle and fractures unevenly or subconchoidally with evidence of two very poor rectangular cleavages, giving fragments which resemble small lumps of "hard" coal. Fragments of sufficient size and purity for specific gravity measurements were not available; however, measurements of three independent fragments of the artificial compound,  $\text{Cu}_3\text{Se}_2$ , gave values,  $G=6.44\text{--}6.49$ , somewhat greater than the value,  $G=5.620$ , given by Klockmann (1891, p. 269) for umangite.

Umangite polishes somewhat unevenly (Fig. 3) and has a characteristic reddish purple colour, not unlike rickardite, the analogous copper telluride described by Thompson (1949, p. 358). Grains of umangite show distinct rectangular outline. Reflection pleochroism is pronounced (reddish purple to greyish blue) somewhat less than that of klockmannite. Anisotropism is very strong (fiery orange to straw-yellow with a rose tint) with four positions of extinction parallel to the poor cleavages. The etch reactions are similar to those given by Short (1940, p. 127):  $\text{HNO}_3$  (1:1) tarnishes to a deep bluish purple;  $\text{HCl}$  (1:1) stains bluish;  $\text{FeCl}_3$ , stains deep blue;  $\text{HgCl}_2$  tarnishes bluish;  $\text{KCN}$ , tarnishes differentially blue to dark grey bringing out grain structure;  $\text{KOH}$ , tarnishes light blue. The Talmadge hardness is B.

Although many fragments with roughly rectangular outline were

tested for single crystal properties, only one fragment with poorly developed cleavages proved in any way satisfactory for single crystal measurements. Fair rotation and Weissenberg photographs were ob-

TABLE 7. UMANGITE— $\text{Cu}_3\text{Se}_2$ : X-RAY POWDER PATTERN  
Orthorhombic,  $P22_12_1$ ;  $a=4.27$ ,  $b=6.39$ ,  $c=12.44$  kX;  $Z=4$

$I$	$\theta(\text{Cu})$	$d(\text{meas.})$	$(hkl)$	$d(\text{calc.})$	$I$	$\theta(\text{Cu})$	$d(\text{meas.})$	$(hkl)$	$d(\text{calc.})$
1	10.35°	4.28	(100)	4.270	8	25.65°	1.776	(220)	1.775
10	12.45	3.57	{(110)	3.550	$\frac{1}{2}$	26.7	1.711	{(017)	1.712
4	13.9	3.20	{(102)	3.520				{(222)	1.707
			{(020)	3.195	1	28.0	1.637	{(223)	1.632
			{(004)	3.110				{(107)	1.641
4	14.35	3.10	{(021)	3.095	$\frac{1}{2}$	28.8	1.596	{(040)	1.597
			{(112)	3.083				{(008)	1.555
2	15.6	2.86	{(022)	2.842	1	29.65	1.554	{(027)	1.553
			{(120)	2.558				{(042)	1.547
3	17.5	2.56	{(023)	2.531				{(311)	1.465
1	18.9	2.37	{(122)	2.366	$\frac{1}{2}$	31.65	1.465	{(232)	1.465
4	19.9	2.26	{(024)	2.229				{(127)	1.460
			{(105)	2.150				{(118)	1.424
			{(200)	2.135	1	32.75	1.421	{(300)	1.423
			{(210)	2.025				{(044)	1.421
3	22.45	2.01	{(032)	2.015				{(233)	1.417
3	23.8	1.905	{(130)	1.906					
9	25.0	1.819	{(132)	1.822					
			{(213)	1.802					

$I$	$\theta(\text{Cu})$	$d(\text{meas.})$	$I$	$\theta(\text{Cu})$	$d(\text{meas.})$	$I$	$\theta(\text{Cu})$	$d(\text{meas.})$
$\frac{1}{2}$	33.6°	1.389	$\frac{1}{2}$	43.9°	1.109	1	54.75°	0.941
1	34.5	1.357	$\frac{1}{2}$	44.5	1.097	$\frac{1}{2}$	57.5	0.911
$\frac{1}{2}$	37.0	1.277	$\frac{1}{2}$	46.15	1.066	$\frac{1}{2}$	58.4	0.902
$\frac{1}{2}$	38.65	1.231	$\frac{1}{2}$	46.95	1.052	$\frac{1}{2}$	60.25	0.885
2	39.8	1.201	$\frac{1}{2}$	47.9	1.036	$\frac{1}{2}$	62.2	0.869
1	40.4	1.186	$\frac{1}{2}$	49.45	1.012	$\frac{1}{2}$	64.0	0.855
1	41.35	1.163	$\frac{1}{2}$	50.35	0.998	$\frac{1}{2}$	69.9	0.818
$\frac{1}{2}$	42.25	1.143	$\frac{1}{2}$	51.35	0.984	$\frac{1}{2}$	75.85	0.793
$\frac{1}{2}$	42.8	1.131	$\frac{1}{2}$	52.75	0.966	$\frac{1}{2}$	80.35	0.780

tained with  $\text{CuK}$  radiation. Measurements on the films gave orthorhombic cell dimensions:

$$a=4.27, b=6.39, c=12.44 \text{ kX}$$

The systematically missing spectra conform to the conditions:  $hkl$  present in all orders,  $0k0$  present only with  $k=2n$ . The extinction condi-

tion in  $00l$  was not determined from Weissenberg photographs but the indexed  $x$ -ray powder pattern suggests  $00l$  present only with  $l=2n$ . These conditions are characteristic of the space group  $P22_12_1$  (class 222).

The cell dimensions of umangite and the measured specific gravity of the compound  $\text{Cu}_3\text{Se}_2$ , combined with the analyses given by Klockmann (1891), indicate the cell content  $\text{Cu}_{12}\text{Se}_8$ . However, the specific gravity of umangite calculated for the unit cell containing  $4[\text{Cu}_3\text{Se}_2]$  is 6.779, higher than the measured value, 6.44–6.49 for the artificial compound. This discrepancy may be due to the voids in the artificial material, but there is also the possibility that umangite, like rickardite (Forman & Peacock, 1949), is a grossly defective compound  $\text{Cu}_{4-x}\text{Se}_2$  only approximating  $\text{Cu}_3\text{Se}_2$  in composition.

Identical  $x$ -ray powder patterns are given by umangite (Fig. 17, Table 7) and pyrosynthetic  $\text{Cu}_3\text{Se}_2$  (Fig. 18). The measured spacings given by Waldo (1935) and Harcourt (1942) agree fairly well with the strong lines of our pattern.

The compound  $\text{Cu}_3\text{Se}_2$  was prepared by fusing copper and selenium metals in appropriate atomic proportions in a vacuum. The resulting regulus is bluish black with a reddish tint and homogeneous, except for a few minute voids. In polished section the product is reddish purple similar to umangite and yields an  $x$ -ray powder pattern identical with umangite.

These observations show that, although umangite ( $\text{Cu}_3\text{Se}_2$ ) and rickardite ( $\text{Cu}_3\text{Te}_2$ ) are physically, chemically and optically similar, they are not isostructural as might be expected. The empirical formula,  $\text{Cu}_3\text{Se}_2$ , suggested by Klockmann (1891) is confirmed by the fact that homogeneous artificial material identical with umangite was formed by fusion of the elements in these proportions.

#### **Clausthalite—PbSe**

Clausthalite, Clausthal, Harz mountains, Germany (ROM, E3120); granular and massive claustralite embedded in a light silicified rock which contains a few grains of chalcocopyrite.

Clausthalite and penroseite, Colquechaca, Bolivia (ROM, M19163); fine grained interstitial claustralite in penroseite with siliceous veinlets and alteration products.

With a hand lens, claustralite is lustrous lead-grey with a faint bluish cast on fresh surfaces, whereas old weathered surfaces are dull greyish black with occasional reddish brown spots. The mineral is brittle and fractures easily showing cubic cleavage, slightly less perfect than galena. Specific gravity measurements on clean, selected, cleavage fragments gave  $G=8.08$ – $8.22$  with the Berman balance.

Clausthalite polishes to a smooth surface broken only by a few triangular pits which are not as distinct as those in galena. The polished surface

is galena-white with a greyish tinge but lighter than tetrahedrite. It is clearly isotropic. The etch reactions are similar to those given by Short (1940, p. 129):  $\text{HNO}_3$  (1:1), tarnishes leaving a brick red coating of selenium;  $\text{HCl}$  (1:1), readily yields a greyish brown stain;  $\text{FeCl}_3$ , tarnishes iridescent;  $\text{KCN}$ , negative;  $\text{HgCl}_2$ , negative;  $\text{KOH}$ , negative. The Talmadge hardness is B.

Clausthalite (ROM, E3120) gave an  $x$ -ray powder pattern (Fig. 21) which is indexed on a cubic lattice with  $a=6.110$  kX; this is distinctly lower than the values,  $a=6.162$  Å given by Olshausen (1925) for clausthalite and  $a=6.14$  Å given by Ramsdell (1925, p. 283) for the artificial

TABLE 8. CLAUSTHALITE—PbSe: X-RAY POWDER PATTERN

Cubic,  $Fm\bar{3}m$ ;  $a=6.110$  kX;  $Z=4$ 

<i>I</i>	$\theta(\text{Cu})$	<i>d</i> (meas.)	( <i>hkl</i> )	<i>d</i> (calc.)	<i>I</i>	$\theta(\text{Cu})$	<i>d</i> (meas.)	( <i>hkl</i> )	<i>d</i> (calc.)
2	12.6°	3.52	(111)	3.527	$\frac{1}{2}$	48.15°	1.032	(135)	1.033
10	14.6	3.05	(002)	3.055	2	49.05	1.018	$\left\{ \begin{matrix} (006) \\ (244) \end{matrix} \right\}$	1.018
9	20.85	2.16	(022)	2.160	2	52.8	0.965	(026)	0.966
5	24.7	1.840	(113)	1.842	2	56.65	0.920	(226)	0.921
5	25.85	1.763	(222)	1.764	$\frac{1}{2}$	60.65	0.882	(444)	0.882
2	30.25	1.526	(004)	1.527	$\frac{1}{2}$	63.95	0.856	$\left\{ \begin{matrix} (117) \\ (155) \end{matrix} \right\}$	0.856
1	33.3	1.400	(133)	1.402	1	65.15	0.847	(046)	0.847
5	34.25	1.366	(024)	1.366	2	70.3	0.816	(246)	0.816
4	38.05	1.247	(224)	1.247	1	75.05	0.796	(137)	0.796
1	40.85	1.175	$\left\{ \begin{matrix} (115) \\ (333) \end{matrix} \right\}$	1.176					
1	45.45	1.079	(044)	1.080					

compound PbSe. Table 8 gives the powder data with measured spacings which agree well with those of Harcourt (1942, p. 77). With 4[PbSe] in the unit cell the calculated specific gravity is  $G=8.28$ , somewhat higher than the measured value,  $G=8.08$ – $8.22$ .

The compound PbSe was prepared by fusing the elements in equal atomic proportions in a vacuum. The components fused readily to a bright metallic globule and cooled to a compact shiny lead-grey regulus showing cubic cleavage. In polished section the product is grey, homogeneous and isotropic, similar to clausthalite. An  $x$ -ray powder pattern (Fig. 22) from a random fragment of this material is identical to that of clausthalite (Fig. 21).

Clausthalite and galena are known to be isostructural, suggesting a solid solution series, PbSe—PbS. In order to test the existence of this series, fusions were made in the standard way at 20 atomic per cent

intervals between the end members and the cube-edges of the products were measured exactly from the back reflection lines.

PbS	20 at. %	40	60	80	PbSe
$a = 5.923$	5.959	6.002	6.038	6.076	6.110 kX

Fig. A gives a plot of the cube-edges and the compositions of the various fusion products. The smooth, almost linear, variation of cube-edge and composition shows that the isostructural compounds PbS and PbSe do in fact form a continuous solid solution series under fusion conditions.

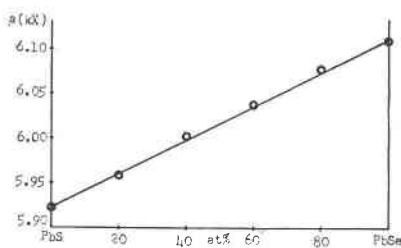


FIG. A. Plot of cube-edge and composition of artificial PbS-PbSe solid solutions.

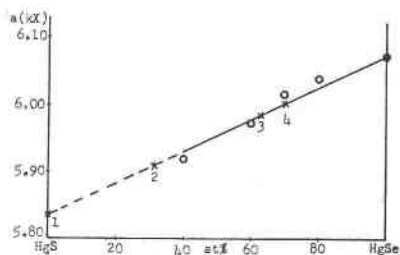


FIG. B. Plot of cube-edge and composition of artificial (circles) and natural (crosses) members of the HgS-HgSe series.

#### Tiemannite—HgSe

Tiemannite, Clausthal, Harz mountains, Germany (ROM, M20129); massive tiemannite separated from chalcopyrite by a calcite-vein, some of the tiemannite has a hard reddish brown coating (not identified).

Tiemannite, Clausthal, Harz mountains, Germany (ROM, M3872); a massive coating on siliceous carbonate rock.

"Onofrite," Pinte County, Utah, U.S.A. (ROM, M20131); a massive ore specimen with a small amount of clayey material.

"Onofrite," Pinte County, Utah, U.S.A. (ROM, M7376); massive in limestone.

In daylight, fresh surfaces of tiemannite are lead-grey with a purplish blue cast and have a metallic sheen not unlike some varieties of chalcocite, while weathered surfaces are dull reddish brown to black. Massive and compact granular tiemannite fractures unevenly to subconchoidally with no evidence of cleavage. Five determinations of the specific gravity, made with the Berman balance on clean fragments gave  $G = 8.24-8.27$ .

In polished section tiemannite is greyish white, slightly darker than clausthalite, and isotropic. The etch reactions are similar to those given by Short (1940, p. 152):  $\text{HNO}_3$  (1:1), negative;  $\text{HCl}$  (1:1), negative;  $\text{KCN}$ , negative;  $\text{FeCl}_3$ , stains greyish brown, rubs off easily;  $\text{HgCl}_2$ , negative;  $\text{KOH}$ , negative. The Talmadge hardness is B.

Tiemannite gave an x-ray powder pattern of the sphalerite type

(Fig. 23, Table 9), which is indexed on a cubic lattice with  $a=6.072$  kX, in good agreement with the value  $a=6.069$  A given by Hartwig (1926). With 4[HgSe] in the unit cell the calculated specific gravity is 8.24, confirming the measured values,  $G=8.24-8.27$ .

The compound HgSe was prepared by fusing the elements in equal atomic proportions in a vacuum. The components fused readily to a bright metallic globule with violent evolution of vapour and cooled to a shiny regulus with some loss of Hg as a mirror sublimate on the wall of the tubes. A section of this material is porous, greyish white and has no

TABLE 9. TIEMANNITE—HgSe: X-RAY POWDER PATTERN  
Cubic,  $F43m$ ;  $a=6.072$  kX;  $Z=4$

<i>I</i>	$\theta$ (Cu)	<i>d</i> (meas.)	( <i>hkl</i> )	<i>d</i> (calc.)	<i>I</i>	$\theta$ (Cu)	<i>d</i> (meas.)	( <i>hkl</i> )	<i>d</i> (calc.)
10	12.7°	3.50	(111)	3.506	1	41.1°	1.169	{(115) (333)}	1.169
2	14.65	3.04	(002)	3.036	1	45.7	1.074	(044)	1.073
*2	15.95	2.80	—	—	2	48.6	1.025	(135)	1.026
8	21.05	2.14	(022)	2.147	$\frac{1}{2}$	53.25	0.959	(026)	0.960
*2	22.75	1.988	—	—	$\frac{1}{2}$	56.1	0.926	(335)	0.926
8	24.85	1.829	(113)	1.831	$\frac{1}{2}$	61.5	0.875	(444)	0.876
$\frac{1}{2}$	26.0	1.754	(222)	1.753	$\frac{1}{2}$	64.85	0.849	{(117) (155)}	0.850
1	30.5	1.515	(004)	1.518	1	71.3	0.811	(246)	0.811
2	33.45	1.394	(133)	1.393	1	76.55	0.790	(137)	0.790
$\frac{1}{2}$	34.55	1.355	(024)	1.358					
2	38.4	1.238	(224)	1.239					

\* Extra lines not identified.

evidence of cleavage. An x-ray powder pattern (Fig. 24) of the product is practically identical to that of tiemannite (Fig. 23).

Since metacinnabar (HgS) is isostructural with tiemannite (HgSe), and onofrite (Dana, 1944, p. 216) has been described as a selenian variety of metacinnabar, Hg(S,Se), a series of Hg—Se—S fusions was made in order to prove or disprove the existence of a solid solution series between the end members, HgSe and HgS. In all, six fusions were made at 20 atomic per cent intervals. X-ray powder patterns of the products gave the sphalerite type of pattern for those fusions with 40 atomic per cent HgSe or more while those with less than 40 atomic per cent gave the cinnabar type of pattern.

Fig. B is a plot of the cube-edges and compositions of the fusion products of sphalerite type (black points) establishing a roughly linear relation. The crossed points represent the cube-edges and compositions, actual or inferred from the curve, of minerals: (1) metacinnabar,

( $a = 5.835$  kX, R. B. Ferguson); (2) onofrite ( $a = 5.906$ , Hartwig, 1926); (3) onofrite (ROM, M7376,  $a = 5.980$  kX, J.W.E.); (4) onofrite (ROM, M20131,  $a = 6.001$  kX, J.W.E.); (5) tiemannite (ROM, M3872, M20129,  $a = 6.072$  kX, J.W.E.).

The plot indicates that there is a metacinnabar-tiemannite series which may be continuous in nature but ranges only from  $\text{HgS}_{60}\text{HgSe}_{40}$  to  $\text{HgSe}$  under fusion conditions. Intermediate members of the series have been called onofrite. Onofrite from Pinte County, Utah, is evidently sulfurian tiemannite, while the mineral measured by Hartwig, in keeping with the analysis of onofrite from San Onofre, Mexico (Dana, 1944, p. 216), is properly called selenian metacinnabar.

#### Klockmannite— $\text{CuSe}$

For a full account of this species see the detailed study of natural and artificial klockmannite which appeared recently in this journal (Earley, 1949).

#### Penroseite— $(\text{Ni,Cu})\text{Se}_2$

Penroseite, Colquechaca, Bolivia (ROM, M18460); massive ore specimen; botryoidal and radiating structures; old surfaces coated with limonite and other alteration products.

Penroseite and clausenthalite, Colquechaca, Bolivia (ROM, M19163); granular to massive penroseite with interstitial clausenthalite showing small siliceous veinlets and brick-red incrustations.

Fresh surfaces of penroseite are steel-grey tarnishing rapidly to a dull lead-grey. Weathered specimens show a brownish coating of limonite or goethite and a brick-red material which was not identified but is comparable to the incrustations of "ahlfeldite" mentioned by Bannister & Hey (1937). The mineral is brittle and fractures with imperfect cubic cleavage or subconchoidally. Although none of the material was entirely suitably for specific gravity measurements due to the many small veinlets of clausenthalite, six measurements of carefully chosen cleavage fragments gave  $G = 6.58-6.74$  with the Berman balance.

A section of penroseite polishes unevenly to a pitted surface and is creamy greyish white, somewhat less lustrous than the intergrown clausenthalite. It is clearly isotropic. The etch reactions are substantially the same as those given by Gordon (1926):  $\text{HNO}_3$  (1:1), stain iridescent subsequently etching a rough grey surface;  $\text{HCl}$  (1:1), negative;  $\text{FeCl}_3$ , negative;  $\text{KCN}$ , greyish brown stain;  $\text{HgCl}_2$ , negative;  $\text{KOH}$ , negative. The Talmadge hardness is  $C+$ , slightly harder than chalcopyrite.

Penroseite (ROM, M18460) gave an  $x$ -ray powder pattern (Fig. 19) of the pyrite type which can be indexed on a cubic lattice with  $a = 5.979$  kX, in fair agreement with the value  $a = 6.001-6.017$  A, given by Ban-



nister & Hey (1937). The measured spacings in Table 11 are essentially the same as those given by Harcourt (1942, p. 93).

Compounds with the gross composition  $(\text{Ni,Cu,Pb})_2\text{Se}$  were prepared by fusing the elements in various atomic proportions in a vacuum. In general, the elements fused with difficulty at high temperatures ( $1000\text{--}1200^\circ\text{C}$ ) to a sinter-like steel-grey mass. However, those fusions containing lead gave small globules of a bright metallic component which proved to be  $\text{PbSe}$  (clausthalite). A polished section of the sinter-like material is similar to penroseite. Table 10 gives the composition of the fusions, the products formed, and the cube-edge of the nickel bearing components.

TABLE 10. Ni-Cu-Pb-Se FUSIONS

Composition of Fusion	Products	Cube-edge of Ni-Component
$\text{NiSe}_2$	$\text{NiSe}_2$	5.945 kX
$(\text{Ni,Pb})\text{Se}_2(10\% \text{ Pb})$	$\text{NiSe}_2 + \text{PbSe}$	5.945 kX
$(\text{Ni,Pb,Cu})\text{Se}_2(12\% \text{ Pb, } 5\% \text{ Cu})$	$(\text{Ni,Cu})\text{Si}_2 + \text{PbSe}$	5.962 kX
$(\text{Ni,Cu})\text{Se}_2(7\% \text{ Cu})$	$(\text{Ni,Cu})\text{Se}_2$	5.979 kX

TABLE 11. PENROSEITE— $(\text{Ni,Cu})\text{Se}_2$ : X-RAY POWDER PATTERNCubic,  $P\bar{a}3$ ;  $a = 5.979$  kX;  $Z = 4$ 

<i>I</i>	$\theta(\text{Cu})$	$d(\text{meas.})$	$(hkl)$	$d(\text{calc.})$	<i>I</i>	$\theta(\text{Cu})$	$d(\text{meas.})$	$(hkl)$	$d(\text{calc.})$
*1	12.5°	3.55	—	—	3	42.0°	1.149	{(115) (333)}	1.150
3	14.8	3.01	(002)	2.990	2	43.9	1.109	{(025) (234)}	1.110
9	16.7	2.67	(021)	2.674	1	44.85	1.090	(125)	1.091
9	18.3	2.45	(112)	2.441	2	46.8	1.054	(044)	1.057
*1	20.85	2.16	—	—	$\frac{1}{2}$	50.6	0.995	(006)	0.996
1	21.3	2.12	(022)	2.114	$\frac{1}{2}$	51.6	0.981	(016)	0.983
$\frac{1}{2}$	22.7	1.992	(003)	1.991	2	52.55	0.968	{(116) (235)}	0.970
* $\frac{1}{2}$	24.65	1.843	—	—	1	57.6	0.910	(335)	0.912
8	25.25	1.802	(113)	1.803	1	59.6	0.891	(036)	0.891
$\frac{1}{2}$	26.55	1.720	(222)	1.726	1	60.7	0.881	(136)	0.881
3	27.6	1.659	(023)	1.658	$\frac{1}{2}$	68.0	0.829	(046)	0.829
4	28.8	1.596	(123)	1.598	1	69.4	0.821	{(027) (146)}	0.821
1	31.0	1.493	(004)	1.494	1	70.9	0.814	{(255) (336)}	0.814
*1	34.4	1.361	—	—					
$\frac{1}{2}$	35.25	1.332	(024)	1.337					
2	36.2	1.301	(124)	1.395					
1	37.1	1.274	(233)	1.275					
$\frac{1}{2}$	39.05	1.220	(224)	1.220					

\* Extra lines due to clausthalite.

These cube-edge values are somewhat smaller than the values,  $a=6.022$  A, given by de Jong & Willems (1928) for artificial  $\text{NiSe}_2$ . Since the addition of Pb produces no change in the cube-edge and results in visible PbSe (clausthalite), Pb apparently does not enter in the composition of penroseite. On the other hand the addition of Cu causes a progressive increase in cube-edge, the compound with 7% Cu (Fig. 20) giving exactly the cube-edge measured on natural penroseite.

From these observations penroseite is cubic as described by Bannister & Hey (1937) and not orthorhombic as suggested by Gordon (1926). The significant amounts of lead found in penroseite by Bannister & Hey (1937) are probably due to intergrown clausthalite.

#### Other Selenides

##### Guanajuatite— $\text{Bi}_2(\text{S},\text{Se})_3$

Two specimens of guanajuatite (ROM, M3773, M3826, Guanajuato, Mexico) are physically and optically similar to bismuthinite. An  $x$ -ray powder pattern (Fig. 25) of guanajuatite (ROM, M3773) shows that this specimen is isostructural with bismuthinite and by analogous indexing gives  $a=11.35$ ,  $b=11.48$ ,  $c=4.04$  kX, as compared to  $a=11.32$ ,  $b=4.17$ ,  $c=11.48$ , all  $\pm 0.02$  A (Ramdohr, 1948a). A series of pyro-synthetic compounds,  $\text{Bi}_2(\text{S}, \text{Se})_3$ , showed that Se can replace S up to  $\text{Se}:\text{S}=1:1$  in the bismuthinite structure.

##### Paraguanajuatite— $\text{Bi}_2\text{Se}_3(?)$

No specimen of this mineral was available for study. Ramdohr (1948a, 1948b, p. 360) states that guanajuatite is paramorphosed in part to rhombohedral *paraguanajuatite* which corresponds to the artificial compound  $\text{Bi}_2\text{Se}_3$  and has a structure similar to that of tellurbismuth  $\text{Bi}_2\text{Te}_3$  and tetradyomite  $\text{Bi}_2\text{Te}_2\text{S}$ . For paraguanajuatite Ramdohr gives hexagonal elements,  $a=4.076$ ,  $c=54.7$  A, which are not very close to  $a=4.125$ ,  $c=28.56$  (R. M. Thompson, *priv. comm.*) for artificial  $\text{Bi}_2\text{Se}_3$ . The  $x$ -ray powder pattern of this compound (Fig. 26) is distinctly different from that of guanajuatite (Fig. 25). Possibly paraguanajuatite with its smaller dimensions,  $a$  and  $c/2$ , carries S and has the composition  $\text{Bi}(\text{Se},\text{S})_3$ .

#### CLASSIFICATION

This study of the mineral selenides largely tends to confirm the classification of these minerals in Danna (1944, p. 157); at the same time it suggests certain modifications.

Under the chemical type  $\text{A}_2\text{X}$  naumannite and aguilarite are appropriately placed with argentite as the non-cubic low temperature  $\beta$ -phases

which have inverted from cubic high temperature  $\alpha$ -phases and have inherited pseudo-cubic crystal forms. The tetragonal or pseudo-tetragonal character of eucairite and crookesite suggest that these minerals might properly be placed in an appropriate sub-group of the  $A_2X$  type. The proof that berzelianite has a defective structure  $Cu_{2-x}Se$  analogous to that of digenite  $Cu_{2-x}S$ , and that these minerals do not exist at the corresponding stoichiometric proportions, indicates the need of a separate  $A_{2-x}X$  type (digenite group).

From the point of view of composition umangite falls in the  $A_3X_2$  group but physically the mineral resembles rickardite whose structural formula is  $Cu_{4-x}Te_2$  with  $x$  nearly 1. Even though umangite is not isostructural with rickardite it is possible that the selenide is a grossly defective compound  $Cu_{4-x}Se_2$ . In this connection it is noteworthy that the  $A_3X_2$  type of Dana is represented only by maucherite with the probably defective structure  $Ni_{11}As_8$ , umangite, and bornite,  $Cu_5FeS_4$ , among which there are no structural relationships and the proportions  $A_3X_2$  are not well shown. The classification of clausthalite, tiemannite, klockmannite and penroseite, is confirmed, and it is shown that onofrite is applicable to intermediate members of a metacinnabar-tiemannite series.

#### CLASSIFICATION OF THE SELENIDE MINERALS

##### $A_2X$ type

*Non-cubic low temperature  $\beta$ -phases (argentite group)*

Naumannite . . . . .  $Ag_2Se$   
 Aguilarite . . . . .  $Ag_4Se_8$

*Tetragonal or pseudo-tetragonal*

Eucairite . . . . .  $AgCuSe$   
 Crookesite . . . . .  $(Cu, Tl, Ag)_2Se$

##### $A_{2-x}X$ type

*Cubic (digenite group)*

Berzelianite . . . . .  $Cu_{2-x}Se$

##### $A_3X_2$ type

*Orthorhombic*

Umangite . . . . .  $Cu_3Se_2$

##### $AX$ type

*Cubic (galena group)*

Clausthalite . . . . .  $PbSe$

*Cubic (sphalerite group)*

Tiemannite . . . . .  $HgSe$   
 Onofrite . . . . .  $Hg(Se, S)$

*Hexagonal (covellite group)*

Klockmannite . . . . .  $CuSe$

##### $AX_2$ type

*Cubic (pyrite group)*

Penroseite . . . . .  $(Ni, Cu)Se_2$

## REFERENCES

- ASTM (1945): X-ray diffraction patterns, first supplementary set of cards—*Am. Soc. Test. Mat.* (Philadelphia).
- BANNISTER, F. A. & HEY, M. H. (1937): The identity of penroseite and blockite—*Am. Mineral.*, **22**, 319–324.
- BORCHERT, W. (1945): Gitterumwandlungen im System  $\text{Cu}_{2-z}\text{Se}$ —*Zeits. Krist.*, **106**, 5–24.
- DANA, E. S. (1892): *System of Mineralogy*, ed. 6—New York.
- DANA, J. D. & E. S. (1944): *System of Mineralogy*, **1**, by C. PALACHE, H. BERMAN & C. FRONDEL—New York.
- DAVEY, W. P. (1923): Berzelianit—*Phys. Rev.*, **21**, 380.
- DE JONG, W. F. & WILLEMS, H. W. V. (1928): Die Verbindungen  $\text{FeSe}_2$ ,  $\text{CoSe}_2$  und  $\text{NiSe}_2$ —*Zeits. anorg. Chem.*, **170**, 241–245.
- EARLEY, J. W. (1949): Studies of natural and artificial selenides: I—Klockmannite,  $\text{CuSe}$ —*Am. Mineral.*, **34**, 435–440.
- FORMAN, S. A. & PEACOCK, M. A. (1949): Crystal structure of rickardite,  $\text{Cu}_{4-z}\text{Te}_2$ —*Am. Mineral.*, **34**, 441–451.
- GORDON, S. G. (1926): Penroseite and trudellite: two new minerals—*Proc. Acad. Nat. Sci. Philadelphia*, **77**, 317–324.
- HARCOURT, G. A. (1942): Tables for the identification of ore minerals by x-ray powder patterns—*Am. Mineral.*, **27**, 63–113.
- HARTWIG, W. (1926): Die Kristallstruktur von Berzelianit—*Zeits. Krist.*, **64**, 503–504.
- HILLER, J. E. (1940): Die Gitterkonstanten von Crookesit, Argyrodit und Canfieldit—*Zbl. Min.*, **A**, 138–142.
- HINTZE, C. (1904): *Handbuch der Mineralogie*, **1**(1)—Leipzig.
- KLOCKMANN, F. (1891): Mineralogische Mittheilungen aus den Sammlungen der Bergakademie zu Clausthal—*Zeits. Krist.*, **19**, 269–272.
- NORDENSKIÖLD, A. E. (1866): Undersökning of selenminerlerierna från Skrikerum—*Svenska Acad. Öfv. Handl.*, **23**, 355–367.
- OLSHAUSEN, S. v. (1925): Strukturuntersuchungen nach der Debye-Scherrer-Methode—*Zeits. Krist.*, **61**, 463–514.
- PEACOCK, M. A. & BERRY, L. G. (1947): Studies of mineral sulpho-salts; XIII—Polybasite and pearceite—*Min. Mag.*, **28**, 1–13.
- RAHLFS, P. (1936): Über die kubischen Hochtemperaturmodifikationen der Sulfide, Selenide und Telluride des Silbers und des einwertigen Kupfers—*Zeits. phys. Chem.*, (B) **31**, 157–194.
- RAMDOHR, P. (1948a): The mineral species guanajuatite and paraganajuatite (*trans.*)—*Comite direct invest recursos mineral. Mèx.*, **Bol.**, **20**, 1–15 [*Chem. Abs.*, **43**, 4979, 1949].
- (1948b): *Klockmann's Lehrbuch der Mineralogie*, ed. 13—Stuttgart.
- RAMSDELL, L. S. (1943): The crystallography of acanthite,  $\text{Ag}_2\text{S}$ —*Am. Mineral.*, **28**, 401–425.
- ROSE, G. (1828): Selenmineralien—*Pogg. Ann.*, **14**, 471–473.
- SCHNEIDERHÖHN, H. & RAMDOHR, P. (1931): *Lehrbuch der Erzmikroskopie*, **2**—Berlin.
- SHORT, M. N. (1940): Microscopic determination of the ore minerals—*U.S.G.S.*, **Bull.** **914**.
- THOMPSON, R. M. (1949): The telluride minerals and their occurrence in Canada—*Am. Mineral.*, **34**, 342–384.
- WALDO, A. W. (1935): Identification of the copper ore minerals by means of x-ray powder diffraction patterns—*Am. Mineral.*, **20**, 575–597.